Title

AktAR and Akt-STOPS: Genetically Encodable Molecular Tools to Visualize and Perturb Akt Kinase Activity at Different Subcellular Locations in Living Cells.

Journal

Current Protocols in Neuroscience, 2(5)

Authors

Zhang, Jin
Zhou, Xin
Mehta, Sohum

Publication Date

2022-05-01

DOI

10.1002/cpz1.416

Peer reviewed

HHS Public Access

Author manuscript

Curr Protoc. Author manuscript; available in PMC 2023 May 01.

Published in final edited form as:

Curr Protoc. 2022 May ; 2(5): e416. doi:10.1002/cpz1.416.

AktAR and Akt-STOPS: Genetically Encodable Molecular Tools to Visualize and Perturb Akt Kinase Activity at Different Subcellular Locations in Living Cells

Xin Zhou[1], **Sohum Metha**[1], **Jin Zhang**[1,2,3,*]

[1]Department of Pharmacology, University of California, San Diego, 9500 Gilman Dr., La Jolla, CA 92093

[2]Department of Chemistry & Biochemistry, University of California, San Diego, 9500 Gilman Dr., La Jolla, CA 92093

[3]Department of Bioengineering, University of California, San Diego, 9500 Gilman Dr., La Jolla, CA 92093

Abstract

The serine/threonine protein kinase Akt integrates diverse upstream inputs to regulate cell survival, growth, metabolism, migration, and differentiation. Mounting evidence suggests that Akt activity is differentially regulated depending on its subcellular location, including the plasma membrane, endomembrane, and nuclear compartment. This spatial control of Akt activity is critical for achieving signaling specificity and proper physiological functions, and deregulation of compartment-specific Akt signaling is implicated in various diseases, including cancer and diabetes. Understanding the spatial coordination of the signaling network centered around this key kinase and the underlying regulatory mechanisms requires precise tracking of Akt activity at distinct subcellular compartments within its native biological contexts. To address this challenge, new molecular tools are being developed, enabling us to directly interrogate the spatiotemporal regulation of Akt in living cells. These include, for instance, the newly developed genetically encodable fluorescent protein-based Akt kinase activity reporter (AktAR2), which serves as a substrate surrogate of Akt kinase and translates Akt-specific phosphorylation into a quantifiable change in Förster resonance energy transfer (FRET). In addition, we developed Akt Substrate Tandem Occupancy Peptide Sponge (Akt-STOPS), which allows biochemical perturbation of subcellular Akt activity. Both molecular tools can be readily targeted to distinct subcellular localizations. Here, we describe a workflow to study Akt kinase activity at different subcellular locations in living cells. We provide a protocol for using genetically targeted AktAR2 and Akt-STOPS, along with fluorescence imaging in living NIH3T3 cells, to visualize and perturb, respectively, the activity of endogenous Akt kinase at different subcellular compartments. We further describe a protocol for using Chemically Inducible Dimerization (CID) to control the plasma membrane-specific inhibition of Akt activity in real time. Lastly, we describe a protocol

[*]Corresponding author. **Jin Zhang** – Department of Pharmacology, Bioengineering, Chemistry & Biochemistry, University of California, San Diego, La Jolla, California 92093, United States. Tel: 001-858-246-0602. jzhang32@ucsd.edu.

CONFLICT OF INTEREST STATEMENT:
The authors declare no conflict of interest.

for maintaining NIH3T3 cells in culture, a cell line known to exhibit robust Akt activity. In all, this approach enables interrogation of spatiotemporal regulation and functions of Akt, as well as the intricate signaling networks in which it is embedded, at specific subcellular locations.

BASIC PROTOCOL 1: Visualizing and Perturbing Subcellular Akt Kinase Activity Using AktAR and Akt-STOPS

BASIC PROTOCOL 2: Using Chemically Inducible Dimerization (CID) to Control Inhibition of Akt at the Plasma Membrane

SUPPORT PROTOCOL 1: Maintaining NIH3T3 cells in culture

Keywords

Live-cell Imaging; Fluorescence; Compartmentalized Signaling; Location-Specific; Protein Kinase B

INTRODUCTION:

The serine/threonine protein kinase B, also known as Akt, is one of the major effectors of phosphoinositide-3-kinase (PI3K) signaling downstream of receptor tyrosine kinases (RTKs) or G-protein-coupled receptors (GPCRs) in mammalian cells (Manning & Toker, 2017). Activation of PI3K leads to production of 3-phosphoinositides (3-PIs), which triggers recruitment to the plasma membrane and subsequent activation of Akt. Active Akt molecules are widely distributed in subcellular compartments, ranging from specific microdomains in the plasma membrane to the nucleus (Sugiyama, Fairn, & Antonescu, 2019). Following activation, Akt acts on over 100 known substrates, directing multiple fundamental cellular functions, including cell survival, growth, metabolism, migration, and differentiation (Manning & Toker, 2017).

The spatiotemporal regulation of Akt activity is essential for the local activation of specific downstream effectors, leading to specific and proper control of cellular processes (Gao et al., 2011; Sugiyama et al., 2019). Disruption of this intricate compartment-specific Akt signaling is implicated in many diseases, such as cancer, diabetes, and neurodegenerative diseases (Sugiyama et al., 2019). For example, plasma membrane-specific Akt regulates formation of protrusions of the plasma membrane, supporting cancer metastasis (Yamaguchi et al., 2011). As such, interrogating the spatiotemporal regulation of Akt networks is critical for advancing our understanding of cell physiology and disease. Investigating this spatiotemporal control, however, requires precise measurements, as well as selective perturbation, of localized Akt activity. These can be difficult or impossible using commonly implemented approaches such as radioactivity or phospho-antibodies-based assays, which measure Akt kinase activity in cell lysates rather than in living cells (Nhu Ngoc Van & Morris, 2013). Furthermore, biochemical purification of subcellular organelles can be challenging as well, as other components of the cells can cofractionate with the organelles-of-interest due to their overlapping biophysical properties and constant interaction with one another (Christopher, Geladaki, Dawson, Vennard, & Lilley, 2022).

Genetically encodable fluorescent protein-based molecular tools, including FRET-based Akt activity reporters (AktARs) (Gao & Zhang, 2008; Zhou et al., 2015) and Akt-specific peptide inhibitors (Maiuri, Ho, & Stambolic, 2010; Zhou, Zhong et al., 2020), in combination with live-cell fluorescence imaging, enable direct visualization and perturbation of Akt kinase activity, with high spatial and temporal resolution within the native cellular contexts (Fig. 1). AktARs serve as substrate surrogates for Akt and translate Akt-specific phosphorylation into a quantitative fluorescent readout. AktAR2, an improved version of AktAR, was developed by sandwiching an Akt substrate peptide derived from Forkhead Box O1 (FoxO1) and an FHA1 phospho-amino acid binding domain (PAABD) between a pair of cyan and yellow fluorescent proteins that can undergo FRET. Specific phosphorylation of AktAR2 by Akt induces binding of the PAABD and the Akt substrate peptide, resulting in a change in FRET between the fluorescent proteins and a corresponding increase in the yellow-to-cyan emission ratio (Fig. 2A and 2B) (Gao & Zhang, 2008; Zhou et al., 2015). To perturb Akt activity at specific subcellular locations, we designed a genetically encodable peptide inhibitor for Akt, Akt Substrate Tandem Occupancy Peptide Sponge (Akt-STOPS). Akt-STOPS was constructed by tagging three tandem repeats of the FoxO1-derived Akt substrate peptide to the C-terminus of a red fluorescent protein (mCherry) (Fig. 2C). The substrate peptide binds to Akt with high affinity, and repeating the amino acid sequence of the substrate peptide allows it to adopt multiple conformations and increases the number of putative binding spots, to facilitate binding (Dudak, Kilic, Demir, Yasar, & Boyaci, 2011; Maiuri et al., 2010). In addition, we incorporated the red fluorescent protein mCherry to display the flexible peptide, as well as to provide a fluorescent marker to confirm Akt-STOPS localization (Zhou, Zhong et al., 2020). Since AktAR2 and Akt-STOPS are genetically encoded, they can be targeted to specific subcellular locations to both monitor and suppress localized Akt activity, respectively (Fig. 2B and 2C).

In this article, we describe a workflow to study Akt kinase activity at different subcellular locations in living cells. Basic Protocol 1 describes the procedure for fluorescence imaging of growth factor-induced Akt activity in living mammalian cells expressing subcellularly targeted AktAR2, either alone or in combination with Akt-STOPS, and includes cell culturing, transfection and starvation, microscope preparation for imaging and acquisition of images and data, and analysis of images and data (Fig. 1, left, and Fig. 3). In Basic Protocol 2, we describe the steps for using a Chemically Inducible Dimerization (CID) system, which drags Akt-STOPS to the plasma membrane upon addition of a small molecule dimerizer (rapamycin or rapalog) at a given time point, to rapidly inhibit local Akt activity (Fig. 1, right, and Fig. 4). The CID system enables more precise temporal control over this highly localized inhibition event (on a timescale of seconds to minutes) compared to the amount of time required to express Akt-STOPS (hours) in Basic Protocol 1 and, thus, offers the possibility to probe downstream signaling events that are temporally correlated with immediate suppression of local Akt activity. Both protocols describe the use of NIH3T3 cells, which are known to exhibit robust Akt activity, as a model system for measuring changes in Akt kinase activity before and after treatment with platelet-derived growth factor (PDGF) (Chan, Rittenhouse, & Tsichlis, 1999; Pekarsky et al., 2001; Pekarsky et al., 2000). Therefore, we also provide Support Protocol 1, for maintaining NIH3T3 cells in culture. A general overview of the workflow is shown in Figure 1.

STRATEGIC PLANNING:

As discussed above, AktARs and Akt-STOPS can be used to interrogate subcellular Akt signaling. As AktARs measure changes in Akt kinase activity in living cells before and after drug treatment, choosing experimental settings that are well-suited for studying Akt signaling ensures robust reporter responses. When setting up an experiment, there are several points to be considered, including the specific cell type for the experiment, treatment conditions for measuring changes in Akt kinase activity, optimal drug concentrations to stimulate or inhibit Akt activity, and the subcellular compartment to be investigated. For example, growth factor and insulin signaling pathways stimulate Akt activity through activation of PI3K (Manning & Toker, 2017). Prior to growth factor or insulin stimulation, cells are incubated in low-serum or serum-free medium, to reduce basal Akt activity (Chan et al., 1999; Franke et al., 1995; Pekarsky et al., 2001; Pekarsky et al., 2000). Akt activity is efficiently induced by PDGF in serum-starved NIH3T3 cells (Chan et al., 1999; Franke et al., 1995; Pekarsky et al., 2001; Pekarsky et al., 2000). Depending on the specific cell type used, conditions for both serum starvation and stimulation should be tested and optimized.

Once the cell type and stimulation conditions have been selected, the next question is which targeted versions of AktAR2 and Akt-STOPS to use, so that the corresponding plasmids can be ordered or generated. Both AktAR2 and Akt-STOPS can be targeted to specific subcellular locations by tagging with well-established subcellular targeting motifs (Zhou, Zhong et al., 2020). For instance, attaching a nuclear localization signal (NLS) (PKKKRKVEDA) to the C-terminus of AktAR2 or Akt-STOPS generates the nuclear-targeted constructs (AktAR2-NLS and Akt-STOPS-NLS), while the plasma membrane-targeted constructs are generated by fusing an N-myristoylation and palmitoylation motif from Lyn kinase (GCIKSKRKDKDP) (Kovarova et al., 2001) to the N-terminus (PM-AktAR2 and PM-Akt-STOPS). AktAR2 can also be targeted to the cytosol by using a nuclear export signal (NES) (EFLPPLERLTL), to monitor cytosolic Akt activity (AktAR2-NES) (Fig. 2B and 2C). To examine whether Akt activity can be induced at different subcellular locations, different growth factors can be tested in different cell types. For example, Akt activity at the plasma membrane can be induced by epidermal growth factor (EGF) in Cos7 and HeLa cells (Miura, Matsuda, & Aoki, 2014), and PDGF stimulates Akt activity at multiple subcellular compartments in NIH3T3 cells, including the plasma membrane (Gao & Zhang, 2008), cytoplasm, and nucleus (Zhou, Zhong et al., 2020). Here, we exemplify the protocols using NIH3T3 cells and PDGF as stimulation for Akt activity.

To introduce plasmids encoding AktAR2 and Akt-STOPS into mammalian cells, a wide range of transfection methods can be used, such as transient transfection and viral transduction. The transfection efficiency is variable for each plasmid, and several factors affect the expression of the constructs in the required cell types; therefore, the transfection parameters need to be tested and optimized in pilot experiments, including transfection methods, total amount of DNA, and the ratio for co-transfected plasmids. Here, we provide our protocols using liposome-mediated transfection of plasmids into NIH3T3 cells. Other transfection methods, such as electroporation or viral infection using viral vectors, can also be used. Notably, for transfection of the CID system in Basic Protocol 2, the amount of PM-FRB expression is limiting for the recruitment of FKBP-Akt-STOPS. Therefore, this

step should be experimentally optimized by varying the plasmid concentrations and ratios of PM-FRB to FKBP-Akt-STOPS during transfection.

Before imaging, it is important to verify that a fluorescence microscope with the appropriate settings is available. In the protocol presented here, we use a standard wide-field microscope, equipped with the appropriate excitation and emission filters for imaging AktAR2 and for monitoring RFP fluorescence of Akt-STOPS. For dual-emission ratio imaging of AktAR2, cells are illuminated at a single wavelength for CFP excitation, and two emission channels are recorded: CFP and YFP. Images are acquired sequentially using a high-speed filter switching wheel, such as Lambda 10–2 filter changer (Sutter Instruments). Alternatively, an emission beam splitting device ("dual-view") can be used to records CFP and YFP images simultaneously. For example, we use a 420DF20 excitation filter, a 450DRLP dichroic mirror, and two emission filters, 475DF40 and 535DF25, for CFP direct (excitation of donor CFP and acquisition of CFP emission) and YFP FRET (excitation of donor CFP and measurement of acceptor YFP), respectively. An optional YFP direct (excitation of acceptor YFP and acquisition of YFP emission) can be used as a control to check for photobleaching (495DF10 excitation filter, 515DRLP dichroic mirror, 535DF25 emission filter). For monitoring RFP fluorescence from Akt-STOPS, we use a 572DF35 excitation filter, a 594DRLP dichroic mirror, and a 645DF75 emission filter. Several online tools can be helpful for choosing filter combinations to image fluorescent proteins, such as the fluorescence spectral viewer (http://www.fpbase.org/spectra)(Lambert, 2019). Control experiments using cells expressing a single fluorescent protein or multiple fluorescent proteins should be performed to make sure filters are appropriate for imaging the desired fluorescent proteins (e.g., CFP, YFP, and RFP). To optimize the fluorescence signal-to-noise ratio and minimize phototobleaching, we typically use neutral-density (ND) filters placed in front of the light source (0.3, 50% transmittance, or 0.6, 25% transmittance), along with 500 ms exposure for CFP and YFP FRET channels, 50 ms exposure for YFP channel, and 100 ms exposure for RFP channel. For the time courses, we acquire a set of images every 30 s, and the time interval can be adjusted to be fast enough to capture the kinase activity dynamics but without too frequent exposure, to avoid photobleaching. In addition, users should select an appropriate objective lens suited for subcellular imaging. For example, higher-magnification objectives (e.g., ≥ 40x) are preferred for visualizing fluorescence signals localized to subcellular structures, such as the plasma membrane. We recommend using a motorized stage with a looping pattern, if available, to enable multi-position imaging and improve imaging efficiency.

BASIC PROTOCOL 1: Visualizing and Perturbing Subcellular Akt Kinase Activity Using AktAR and Akt-STOPS

The following protocol describes the use of the FRET-based Akt activity reporter 2 (AktAR2) and Akt-STOPS that are genetically targeted to specific subcellular locations to track and perturb, respectively, Akt activity in NIH3T3 cells, in response to PDGF stimulation (Chen, Sun, Zhong, Zhou, & Zhang, 2021; Gao & Zhang, 2008; Zhou, Zhong et al., 2020). Briefly, NIH3T3 cells are transfected with plasmid DNA encoding AktAR2, either alone, to assess cellular Akt activity induced by growth factors, or in combination

with Akt-STOPS, to evaluate the inhibition of Akt activity by Akt-STOPS. NIH3T3 cells are then serum-starved to both reduce basal Akt activity and facilitate acute Akt activation upon growth factor stimulation (Franke, Kaplan, Cantley, & Toker, 1997; Zhou et al., 2015; Zhou, Zhong et al., 2020). Then, the microscope is prepared for the imaging experiment, followed by the acquisition of a time series of fluorescence intensity images. During imaging, Akt activity is induced by growth factor stimulation in serum-starved NIH3T3 cells, which results in changes in AktAR2 fluorescence that are recorded across time as a set of image series (e.g., one series per channel). Finally, the image series are analyzed to quantify the changes in fluorescence as a proxy for changes in Akt activity. The following protocol describes imaging using 35-mm glass-bottom dishes.

Materials:

NIH3T3 fibroblasts (ATCC, 30–2030), plated on sterile 35-mm glass-bottom dishes (**see Support Protocol 1**)

Dulbecco's Modified Eagle's Medium (DMEM, Gibco/BRL, 11885) for serum-starvation of NIH3T3 cells

Opti-MEM I Reduced Serum Medium (Gibco, 31985070)

Lipofectamine 2000 (Invitrogen, 11668019)

10–20 μg plasmid DNA encoding AktAR2 and AktAR2 targeted to subcellular locations:

Untargeted Akt activity reporter (AktAR2, Addgene, 64932);

Plasma membrane Akt activity reporter (PM-AktAR2, Addgene, 175013);

Cytosolic Akt activity reporter (AktAR2-NES, Addgene, 175011);

Nuclear Akt activity reporter (AktAR2-NLS, Addgene, 175012).

10–20 μg plasmid DNA encoding Akt-STOPS and Akt-STOPS targeted to subcellular locations:

Untargeted Akt-STOPS (Addgene, 175006);

Plasma membrane Akt-STOPS (PM-Akt-STOPS, Addgene, 175009);

Nuclear Akt-STOPS (Akt-STOPS-NLS, Addgene, 175007).

HBSS imaging buffer (**see** REAGENTS AND SOLUTIONS)

Immersion oil Immersol 518F Fluorescence free (Carl Zeiss, 444960)

Clay

Sterilized microcentrifuge tubes

PDGF stock solution: 50 μg/mL PDGF-BB (Sigma-Aldrich, P4056) in H_2O, with 4 mM HCl and 0.1% BSA.

Inverted fluorescence microscope with appropriate objective, filters/mirrors, detector, and image acquisition software; for example:

Light source (e.g., XBO 75W xenon arc lamp, Carl Zeiss)

Zeiss Axio Observer Z1 microscope (Carl Zeiss)

40x/1.3-NA oil-immersion objective lens

Dichroic mirrors, excitation filters (CFP, YFP, RFP), emission filters (CFP, YFP, RFP)

Cooled charge-coupled device (CCD) camera (e.g., Photonmetrics Evolve 512 EMCCD)

Definite Focus 2 system (Carl Zeiss)

Lambda 10–2 filter changer (Sutter Instruments)

METAFLUOR 7.7 imaging software (Molecular Device)

Computer to run microscope

Other analysis software:

Spreadsheet application (e.g., Microsoft Excel);

Statistical analysis software such as GraphPad Prism 8.

Protocol Steps

Cell Transfection and Starvation

Day 1 (Timing: 30 min)

1. Seed NIH3T3 cells on a 35-mm glass-bottom dish and culture cells at 37 °C under 5% CO_2 to reach 40–60% confluency at the time of transfection (**see SUPPORT PROTOCOL 1**) (Fig. 1A). We recommend at least two technical replicates per experiment, and at least three independent experimental repeats performed on different days. Thus, seed cells on two dishes for each transfection: AktAR2 alone, and AktAR2 with Akt-STOPS.

Day 2 (Timing: 30 min-1 h)

2. Prepare DNA solution: in a microcentrifuge tube, and for each dish, prepare a 1:1 mixture of AktAR2 (0.4 μg): Akt-STOPS (0.4 μg) plasmid DNA, totaling 0.8 μg, and add Opti-MEM to bring the total volume to 50 μL. For monitoring Akt activity only, mix 0.8 μg of plasmid DNA encoding AktAR2 with Opti-MEM in a total volume of 50 μL. Gently mix the plasmid DNA with Opti-MEM. Opti-MEM should only be handled under sterile conditions, such as in a tissue culture hood.

For monitoring and perturbing subcellularly localized Akt activity, use AktAR2 or Akt-STOPS targeted to specific subcellular compartments (Fig. 1B, left and Fig. 2B–C, See Strategic Planning). Here, as an example, PM-Akt-STOPS and Akt-STOPS-NLS are used to inhibit Akt activity at the plasma membrane and the nucleus, respectively. AktAR2 targeted to the plasma membrane (PM-AktAR2), the nucleus (AktAR2-NLS), or the cytosol (AktAR2-NES) is used to assess the specificity and selectivity of Akt inhibition by Akt-STOPS.

3. Prepare Lipofectamine solution: for each transfection reaction from step 2, and in a separate tube, mix 2 μL of Lipofectamine 2000 with Opti-MEM for a total volume of 50 μL and incubate at room temperature for 5 min.

4. For each transfection, add all (50 μL) of the Lipofectamine solution dropwise to the DNA solution (Step 2) and pipet gently to mix. Incubate for 20 min at room temperature.

Mix the Lipofectamine/DNA solution gently and do not vortex.

5. In a tissue culture hood, and for each dish prepared in Step 1, replace the cell culture medium with 2 mL of pre-warmed serum-free DMEM. Add each (100 μL) Lipofectamine/DNA solution from step 4 dropwise to the corresponding dish and rock each dish gently back and forth to evenly disperse the transfection reagents. Incubate cells at 37 °C under 5% CO_2 for 21–24 h.

Optimize the amounts of transfection components according to the manufacturer's instructions, if necessary. Verify reporter expression in the transfected cells on a fluorescence microscope as early as 18 hr after transfection, if possible. Since adding localization signals to GFP decreases its maximum expression level (Mori, Yoshida, Satoh, & Moriya, 2020), it may be necessary to increase the amount of transfected DNA, relative to untargeted constructs, for subcellularly targeted constructs. For example, use 1.2 μg per dish (instead of 0.8 μg) for expressing subcellularly targeted AktAR2 alone, and use 0.6 μg of subcellularly targeted AktAR2 and 0.6 μg of Akt-STOPS for co-expressing (totaling 1.2 μg) per dish.

Microscope Preparation (Timing: 10 min)

Day 3

6. Turn on the lamp, definite focus, microscope, filter changer, camera, and computer. Load the METAFLUOR imaging software and either configure or load a protocol within METAFLUOR to acquire a time series of images for the FRET, CFP, YFP, and RFP channels. RFP (mCherry) images are acquired to verify the expression and localization of Akt-STOPS. Ensure that the filter configuration and acquisition protocol are appropriate for the experiment by exciting the fluorophores and examining the emitted fluorescence (Waters, 2009). Example filter sets for the individual channels are:

   FRET — 420DF20 excitation filter, 450DRLP dichroic mirror, 535DF25 emission filter.

CFP — 420DF20 excitation filter, 450DRLP dichroic mirror, 475DF40 emission filter.

YFP — 495DF10 excitation filter, 515DRLP dichroic mirror, 535DF25 emission filter.

RFP — 568DF55 excitation filter, 600DRLP dichroic mirror, 653DF95 emission filter.

7. Aspirate the serum-free DMEM from the side of the 35-mm glass-bottom imaging dish containing serum-starved NIH3T3 cells, with minimal agitation to the cells. Wash cells with 1 mL of HBSS imaging buffer by adding along the side of the dish, to avoid disturbing the cells. Then, replace with 1 mL of fresh HBSS imaging buffer. Gently rock the dish side to side and avoid pipetting directly over the cells.

8. Place a drop of immersion oil on the 40x objective and securely mount the imaging dish on the microscope stage using clay. Bring cells into focus using the brightfield setting, then switch to fluorescence mode to select transfected cells. Typically, only a fraction of cells are transfected in a given field of view. Depending on the size of field of view, select an area containing 1–5 cells exhibiting healthy morphology, clear probe expression, and proper cellular distribution of AktAR2 and Akt-STOPS (**see** Critical Parameters).

Following serum starvation, it is expected that a subset of cells will undergo growth arrest and apoptosis (Kulkarni & McCulloch, 1994; Pirkmajer & Chibalin, 2011). Therefore, it is important to select healthy NIH3T3 cells for imaging that appear fibroblast-like and have elongated shapes, rather than being balled-up or rounded (Fig. 3A). In addition, ensure that the imaged cells have intermediate-to-high fluorescence intensities. Too-high intensities due to overly high expression of the kinase reporter could raise the possibility of perturbation of endogenous signaling pathways, as well as potential phototoxicity, whereas too-low intensities may lead to reduced signal-to-noise ratios. Usually cells with too-high fluorescent signals can sometimes shrink quickly during imaging. Cells are considered too dim if the fluorescent images are not clearly distinguishable from the background. Depending on exposure times, ND filter(s) used, and camera setting, intermediate-to-high fluorescence intensities range from about 2%–13% of the dynamic range of the camera. Furthermore, select cells with proper cellular distribution of fluorescence. For untargeted AktAR2, the yellow and cyan fluorescence signals should be uniformly and evenly distributed throughout the cells. Similarly, Akt-STOPS should exhibit red fluorescence throughout the cells. For AktAR2 and Akt-STOPS with subcellular targeting, selected cells should exhibit well-localized fluorescence that matches the expected subcellular targeting. For example, plasma membrane targeted AktAR2 or Akt-STOPS should display distinct CFP/YFP fluorescence or RFP fluorescence only at the cell periphery. For cytosolic or nuclear targeted constructs, select cells that show distinct fluorescence exclusively in the cytoplasm or nucleus, respectively (Fig. 3A).

Image and Data Acquisition *(Timing: ~1 hr per dish)*

9. Use the imaging software (e.g., METAFLUOR) to set the exposure time for each individual channel. For AktAR2 and Akt-STOPS, typical exposure times for FRET, CFP, YFP, and RFP are 500, 500, 50, and 100 ms, respectively, though these values can be adjusted based on expression levels and microscope components.

It is critical to optimize the excitation/exposure time, since long exposure times increase the potential for photobleaching and phototoxicity, whereas short exposure times result in poor signal-to-noise ratio. In addition, time interval should be adjusted to be fast enough to capture the Akt kinase activity dynamics while avoiding too frequent excitation exposure.

10. Acquire the first set of images in step 8 for each channel (e.g., FRET, CFP, YFP, and RFP, acquired sequentially at each time point). The imaging software METAFLUOR allows real-time processing of ratio changes, providing instant feedback on the experiment. To monitor the changes in emission ratio in real time, use METAFLUOR and draw regions of interest (ROIs) for each fluorescent cell in the field, and, as a background region, choose a region where no transfected cells or no cells are present.

11. Begin acquiring a time series of images of the field-of-view chosen in Step 8 for each channel (e.g., FRET, CFP, YFP, and RFP, acquired sequentially at each time point). Use the imaging software (e.g., METAFLUOR) to set the time lapse interval between each set of acquisitions. Images are typically taken every 30 sec. Log the fluorescence intensities (arbitrary units, a.u.) from each channel for each ROI acquired during the experiment.

12. Stimulate Akt activity. Acquire 6–10 sets of images in order to establish a baseline (generally 3 to 5 min, or until the baseline of emission ratios appears flat and stable by monitoring METAFLUOR real-time processed ratios). Then, remove about one third of the imaging buffer, typically 300 μL, from the imaging dish and add it directly to a microcentrifuge tube containing 1 μL of PDGF (stock concentration: 50 μg/mL). Mix, and then gently add this mixture back to the imaging dish (final concentration: 50 ng/mL PDGF) by pipetting up and down at least three times to the side of the dish to ensure homogenous distribution of the drug, being careful not to disturb the cells or move the dish. Continue acquiring the image series every 30 s for about 30 min, or until the fluorescence change reaches a steady plateau, to capture the stimulated response.

Akt-specific inhibitors (e.g., GDC-0068 and MK-2206) can be subsequently added to examine whether the response is specific to Akt kinase activity.

When measuring changes in kinase activity using AktAR2, it is important to establish the effective concentrations of the drugs used to stimulate (e.g., PDGF) or inhibit (e.g., GDC-0068 and MK-2206) the kinase. Pretreatment with Akt inhibitors before PDGF stimulation can be carried out to validate the specificity of the response of AktAR2.

Images and Data Analysis *(Timing: ~15 min per dish)*

Day 4

13. Using the imaging software of choice, carefully re-draw regions of interest (ROIs) for each fluorescent cell in the field, and a background region, as in Step 11. Log the fluorescence intensities (arbitrary units, a.u.) from each channel for each ROI acquired frame-by-frame, and carefully track the ROIs during the time course.

For analysis of untargeted reporters, whole-cell ROIs are used. To analyze subcellularly targeted AktAR2, ROIs at given subcellular regions, such as the plasma membrane, cytosol, or nucleus, are used. For example, use ROIs at the cell periphery for analysis of plasma membrane-targeted AktAR2 based on CFP fluorescence image of the reporter. For cytosolic or nuclear AktAR2, use ROIs in the respective regions of cytoplasm or the nucleus based on YFP fluorescence image. Image and quantify about 20–30 cells across at least three independent experiments (e.g., 2–3 independent 35-mm imaging dishes across different cell preparations) per condition.

14. Export the data to a spreadsheet (e.g., Excel file) and calculate the FRET emission ratio (R) (yellow-to-cyan) at each time point using the logged emission intensity data and the following equation:

$$R\left(Y/C\right) = \frac{FRET\ intensity\ of\ ROI - FRET\ intensity\ of\ Background}{CFP\ intensity\ of\ ROI - CFP\ intensity\ of\ Background}$$

15. Set the time point immediately before drug addition as time 0. Normalize the time courses from step 14 by dividing the ratios (R) at each time point by the ratio at time 0 (R_0) (alternatively, calculate the average emission ratio of the baseline to use for normalization), and plot the normalized yellow-to-cyan emission ratio (R/R_0) versus time. Data can be plotted as single-cell time courses to visualize cell-to-cell variations, or the normalized ratio (R/R_0) for all cells can be averaged and plotted as the mean and SEM using GraphPad Prism or any other statistical software of choice (Fig. 3B and 3D). For biosensor responses, calculate the maximum ratio changes ($\Delta R/R_0$) as $(R_{max} - R_0)/R_0$, where R_{max} is the maximum ratio value recorded after stimulation, and R_0 is the ratio value at time 0 min. Convert the biosensor responses ($\Delta R/R_0$) into percentage (%), and perform statistical analyses as desired (e.g., right panels in Fig. 3C and 3E; see Understanding Results).

For a defined location where Akt activity is detected using subcellularly targeted AktAR2, Akt-STOPS targeted to the same location can then be co-expressed with AktAR2 to examine whether local Akt activity is efficiently perturbed by local Akt-STOPS. As a control, AktAR2 targeted to locations other than where Akt activity is being perturbed can be imaged to examine specificity.

BASIC PROTOCOL 2: Using Chemically Inducible Dimerization (CID) to Control Inhibition of Akt at the Plasma Membrane

To control the location-specific inhibition of Akt signaling at a desired time point, users can employ Chemically Inducible Dimerization (CID), which can be utilized as a powerful approach to induce translocation of protein-of-interest, for example, Akt-STOPS, to the plasma membrane upon addition of the dimerizer (Ross, Mehta, & Zhang, 2017; Voss, Klewer, & Wu, 2015). This approach allows additional temporal control of the inhibition events, at the given time point when the dimerizer is added. A typical CID system is based on the rapamycin-induced dimerization between FK506 binding protein (FKBP) and FKBP12-rapamycin binding domain (FRB) (Bayle et al., 2006; Inoue, Heo, Grimley, Wandless, & Meyer, 2005; Mabe, Nagamune, & Kawahara, 2014). To inhibit plasma membrane Akt activity using CID, Akt-STOPS is tagged with FKBP (FKBP-Akt-STOPS), and FRB is targeted to the plasma membrane using a targeting motif derived from Lyn kinase (PM-FRB) (Fig. 4A). Addition of the dimerizer, either rapamycin or rapalog (Bayle et al., 2006), induces formation of the FKBP-FRB heterodimer, which rapidly recruits Akt-STOPS and inhibits Akt activity at the plasma membrane (Fig. 4B). Here, we describe a method to use CID to rapidly modulate Akt activity specifically at the plasma membrane, allowing dissecting downstream signaling networks resulting from acute inhibition of highly localized Akt signaling.

Materials:

NIH3T3 fibroblasts (ATCC, 30–2030), plated on sterile 35-mm glass-bottom dishes (**see Support Protocol 1**)

Dulbecco’s Modified Eagle’s Medium (DMEM, Gibco/BRL, 11885) for serum-starvation of NIH3T3 cells

Opti-MEM I Reduced Serum Medium (Gibco, 31985070)

Plasmid DNA encoding PM-FRB and FKBP-Akt-STOPS (available upon request from Zhang lab)

Lipofectamine 2000 (Invitrogen, 11668019)

Rapamycin stock solution 100 μM (LC Labs, R-5000)

Rapalog AP21967 (optional, stock solution 3 μM, Takara Bio, 635067)

HBSS imaging buffer (**see** REAGENTS AND SOLUTIONS)

Immersion oil Immersol 518F Fluorescence free (Carl Zeiss, 444960)

Clay

Sterilized microcentrifuge tubes

PDGF stock solution: 50 μg/mL PDGF-BB (Sigma-Aldrich, P4056) in H_2O, with 4 mM HCl and 0.1% BSA.

Inverted fluorescence microscope with appropriate objective, filters/mirrors, detector, and image acquisition software; for example:

Light source (e.g., XBO 75W xenon arc lamp, Carl Zeiss)

Zeiss Axio Observer Z1 microscope (Carl Zeiss)

40x/1.3-NA oil-immersion objective lens

Dichroic mirrors, excitation filters (CFP, YFP, RFP), emission filters (CFP, YFP, RFP)

Cooled charge-coupled device (CCD) camera (e.g., Photonmetrics Evolve 512 EMCCD)

Definite Focus 2 system (Carl Zeiss)

Lambda 10–2 filter changer (Sutter Instruments)

METAFLUOR 7.7 imaging software (Molecular Device)

Computer to run microscope

Other analysis software:

Spreadsheet application (e.g., Microsoft Excel);

Statistical analysis software such as GraphPad Prism 8.

Protocol Steps

Cell Transfection and Starvation

Day 1 (Timing: 30 min)

1. Seed NIH3T3 cells on sterile 35-mm glass-bottom dishes and culture cells at 37 °C under 5% CO_2 to reach 40–60% confluency at the time of transfection (**see SUPPORT PROTOCOL 1**) (Fig. 1A). We recommend at least two technical replicates per experiment, and at least three independent experimental repeats performed on different days. In addition, suitable control experiments should include no FRB expression and treatment with DMSO rather than dimerizer. Thus, seed cells on two dishes for each transfection:
    a. Negative control 1: PM-AktAR2 + PM-FRB + FKBP-Akt-STOPS, treated with PDGF followed by DMSO;
    b. Negative control 2: PM-AktAR2 + FKBP-Akt-STOPS (no FRB expression), treated with PDGF followed by dimerizer;
    c. Negative control 3: PM-AktAR2 + PM-FRB, treated with PDGF followed by dimerizer;

d. PM-AktAR2 + PM-FRB + FKBP-Akt-STOPS, treated PDGF followed by with dimerizer.

Day 2 (Timing: 30 min- 1h)

2. Prepare DNA solution:

For each co-transfection of three plasmids, and in a microcentrifuge tube, prepare a 1:2:1 mixture of PM-AktAR2 (0.4 μg): PM-FRB (0.8 μg): FKBP-Akt-STOPS (0.4 μg) plasmid DNA, totaling 1.6 μg, and add Opti-MEM to bring the total volume to 100 μL.

For each transfection with two plasmids, and in a microcentrifuge tube, prepare a 1:1 mixture of PM-AktAR2 (0.4 μg): FKBP-Akt-STOPS (0.4 μg) plasmid DNA, totaling 0.8 μg, and add Opti-MEM to bring the total volume to 50 μL.

3. Gently mix the plasmid DNA with Opti-MEM. Opti-MEM should only be handled under sterile conditions, such as in a tissue culture hood.

Because transfection efficiency varies for different cell types, plasmids, incubation time, total amount of DNA, and the ratio of different plasmids, different ratios of FRB/FKBP for co-transfection need to be optimized in pilot experiments.

4. Prepare Lipofectamine solution:

For each co-transfection of three plasmids, and in a separate tube, mix 4 μL of Lipofectamine 2000 with Opti-MEM for a total volume of 100 μL. For each co-transfection of two plasmids, and in a separate tube, mix 2 μL of Lipofectamine 2000 with Opti-MEM for a total volume of 50 μL. Incubate at room temperature for 5 min.

5. For each co-transfection of three plasmids, add all (100 μL) of the Lipofectamine solution dropwise to the DNA solution and pipet gently to mix. For each co-transfection of two plasmids, add all (50 μL) of the Lipofectamine solution dropwise to the DNA solution and pipet gently to mix. Incubate for 20 min at room temperature. Mix the Lipofectamine/DNA solution gently and do not vortex.

6. In a tissue culture hood, and for each 35-mm glass-bottom dish containing NIH3T3 cells prepared in Step 1, replace the medium with 2 mL of pre-warmed serum-free DMEM medium. For each co-transfection of three plasmids, add all (200 μL) of the Lipofectamine/DNA solution dropwise to the proper dish. For each co-transfection of two plasmids, add all (100 μL) of the Lipofectamine/DNA solution dropwise to the proper dish. Rock the dish gently back and forth to evenly disperse the transfection reagents.

Microscope Preparation, Image and Data Acquisition

Day 3 (Timing: 10 min + 1h per dish)

7. Proceed with steps 6–11 of Basic Protocol 1 for preparation and setup of the microscope for imaging. Depending on the size of field-of-view, select 1–5 suitable cells to image. These cells should exhibit the appropriate healthy morphology, clear probe expression, and proper cellular distribution for PM-AktAR2 (intermediate-to-high intensity levels of YFP or CFP at the cell periphery) and FKBP-Akt-STOPS (red fluorescence in the cytoplasm) (**see** Critical Parameters).

8. Stimulate Akt activity and inhibit plasma membrane Akt activity. To do this, acquire 6–10 sets of images in order to establish a baseline (generally 3 to 5 min, or until a stable, flat baseline is observed by monitoring METAFLUOR real-time processed ratios). Remove about one third of imaging buffer, typically about 300 μL, from the imaging dish and add to a microcentrifuge tube containing 1 μL of PDGF (stock concentration: 50 μg/mL). Mix and gently add this mixture back to the imaging dish (final concentration: 50 ng/mL PDGF) by pipetting down along the side of the dish, being careful not to disturb the cells. Pipet carefully to evenly mix the drug throughout the dish. Continue acquiring the image series every 30 s for about 10 min to capture the stimulated response (PM-AktAR2 response is faster than diffusive AktAR2).

9. To induce the plasma membrane translocation of Akt-STOPS, remove about 300 μL of imaging buffer from the imaging dish and add to a microcentrifuge tube containing 1 μL of rapamycin (stock concentration: 100 μM). Mix well. Mix and gently add this mixture back to the imaging dish (final concentration: 100 nM rapamycin) by pipetting down the side of the dish, being careful not to disturb the cells. Pipet carefully to evenly mix the drug throughout the dish. Continue acquiring the image series every 30 s for about 20 min to capture the reversal of the response.

Alternatively, add rapamycin analogue, Rapalog (AP21697), to induce dimerization. The presence of the T2098L mutation in the FRB fragment used in this study allows for the use of rapalog AP21967 that does not cross-react with the wildtype, endogenous FRB domain of mTOR. Establish effective concentrations of rapamycin or rapalog in the cells to be studied in pilot experiments. For NIH3T3 cells, we use 3 μM rapalog (AP21697) or 100 nM rapamycin for efficient recruitment (Zhou, Zhong et al., 2020). The induced translocation of Akt-STOPS is typically rapid, on a timescale of seconds to minutes, and in current systems, it is essentially irreversible. Establish time-lapses by observing both the changes in Akt-STOPS translocation and the reversal of the AktAR2 reporter response.

Images and Data Analysis

Day 4 (Timing: ~ 15 min per dish)

10. Proceed with steps 13–15 of Basic Protocol 1 for images and data analysis. Sample data is shown in Figure 4C and discussed in “Understanding Results”

To better visualize certain features of spatiotemporal control of Akt activity, for example, the increase and decrease in Akt activity at the plasma membrane before and after recruitment of Akt-STOPS to the plasma membrane, pseudocolor images for each acquisition can also be generated using the METAFLUOR software to indicate the yellow-to-cyan emission ratio, where warmer colors represent high Y/C emission ratio and high Akt activity, and cooler colors represent low Y/C emission ratio and low Akt activity (PM-AktAR2, upper panel, Figure 4C, Movie S1).

SUPPORT PROTOCOL 1: Maintenance of NIH3T3 cells in culture

The protocol below outlines the procedure for passaging NIH3T3 cells, both for prolonged maintenance and for use in the imaging experiments described in the Basic Protocol 1 and Basic Protocol 2.

Materials:

NIH3T3 cells (American Type Culture Collection, 30–2030)

70% Ethanol (EtOH)

Dulbecco's Phosphate Buffered Saline without Ca^{2+} or Mg^{2+} (DPBS, Gibco, 14190–144)

NIH3T3 cell culture medium (**see** Reagents and Solution)

0.25% Trypsin/ethylenediamine tetraacetic acid (EDTA) solution (Gibco, 25200–056)

Tissue culture incubator

Tissue culture hood

Tissue culture flasks (e.g., T-25 cm^2, BD Falcon)

35-mm glass-bottom imaging dishes (e.g., CellVis, D35–14-1.5-N)

Protocol steps:

1. Maintain NIH3T3 cells in 5 mL of NIH3T3 cell culture medium in T-25 cm^2 flasks in a humidified, 37 °C incubator with a 5% CO_2 atmosphere.. Passage cells whenever they reach 50 to 70% confluence as observed under a standard tissue culture microscope. The NIH3T3 cells should not be allowed to become completely confluent.

   For NIH3T3 cell culture medium, we recommend calf serum instead of fetal bovine serum (**see** Reagents and Solution)

2. Before removing NIH3T3 cells from the incubator for passaging, sterilize work surfaces in the tissue culture hood using 70% ethanol and make sure that all required supplies are at hand, including pipets, pipet tips, flasks, media aliquots, dishes, etc., and are sterile and available in the hood before beginning.

3. Examine the cells under a microscope to check cell confluency and morphology. Healthy NIH3T3 cells should appear fibroblast-like, with elongated shapes, rather than being balled-up or rounded. Carefully transfer the T-25 cm^2 flask to the hood.

4. Remove the culture medium from the flask. Gently wash twice with 2 mL of DPBS without calcium and magnesium to remove all traces of serum.

5. Pipet 300 μL of trypsin/EDTA solution into the flask, and gently rock the flask back and forth several times. Let sit for 1 to 2 min, until 90% of cells begin to disperse (round up) as observed under a microscope.

6. Add 4.7 mL of fresh, pre-warmed NIH3T3 cell culture media to the flask and suspend the cells by gently pipetting up and down. Avoid over-pipetting, as this could damage the cells.

7. Perform a 1:6 split (800 μL cell suspension) of culture into a new T-25 flask containing 5 mL of pre-warmed NIH3T3 cell culture media, to maintain the cells. Depending on the surface areas of tissue culture plates/flasks, inoculating $3–5 \times 10^3$ cells/cm^2 is recommended. Split cells every two or three days.

8. For imaging experiments (Basic Protocol 1 and Basic Protocol 2), perform a 1:3 split (600 μL cell suspension) of cells into 35-mm glass-bottom dishes containing 2 mL of pre-warmed NIH3T3 cell culture media.

   Cells should reach 40–60% confluency after approximately 24 hr and should be transfected at this confluency, as stated in Basic Protocol 1 and Basic Protocol 2.

REAGENTS AND SOLUTIONS:

All solutions should be made using water with 18.2 MΩ-cm resistivity, and prepared under sterile conditions in a tissue culture hood.

HBSS imaging buffer

1x Hank’s Balanced Salt Solution (made from 10x HBSS (Gibco, 14065))

20 mM HEPES (Invitrogen, 15630080)

2.0 g/L D-glucose (Sigma, G8769)

Adjust pH to 7.4 with sodium hydroxide (NaOH), then filter sterilize using a 0.22 μm filter. Store a 50-mL aliquot at room temperature near the microscope and store the remainder at 4 °C.

NIH3T3 cell culture medium

Dulbecco’s Modified Eagle’s Medium, 1 g/L glucose (Gibco, 11885084)

10 % (v/v) calf serum (CS, ATCC, 302030)

1% penicillin-streptomycin (Sigma-Aldrich, P4333)

Store culture media at 4 °C and warm to 37 °C before using with cells.

COMMENTARY:

BACKGROUND INFORMATION

Akt regulates many fundamental cellular processes through its kinase activity. The signaling specificity of Akt is guided by its wide distribution in cells, ranging from microdomains within the plasma membrane, to endomembranes and nuclear compartments. The spatial compartmentalization of Akt activity and function is essential for the regulation of a wide range of physiological processes in many different cell types and tissues, including cell survival, growth, and metabolism (Manning & Toker, 2017; Sugiyama et al., 2019). Consistent with its widespread cellular roles, disruption of compartmentalized Akt signaling networks underlies numerous diseases, such as cancer and type 2 diabetes (Manning & Toker, 2017; Sugiyama et al., 2019).

Unraveling the detailed molecular wiring of Akt signaling in real time within its native environment requires the development of biochemical, cell biological, and systems biology approaches. Commonly implemented approaches for probing Akt activity rely on quantitative radiography measurements or phosphorylation-specific antibodies using cell lysates, which do not allow for real-time analysis of Akt activity in the native cellular context (Nhu Ngoc Van & Morris, 2013). To address this, fluorescent peptide sensors for Akt have been developed, such as sensors based on synthetic peptide substrates containing sulfonamide-oxine (Sox) chromophores. Upon phosphorylation of the Sox-containing peptide, the chromophore binds Mg^{2+} and undergoes chelation-enhanced fluorescence (CHEF), allowing for direct, rapid, and continuous detection of Akt kinase activity in crude cell or tissue lysates, as well as in living cells (Lukovic, Gonzalez-Vera, & Imperiali, 2008; Shults, Carrico-Moniz, & Imperiali, 2006; Shults, Janes, Lauffenburger, & Imperiali, 2005). Although these fluorescent peptide sensors allow versatile experimental designs and applications, their use in living cells requires efficient cellular uptake. This limitation can be addressed by introducing cell-penetrating peptides or liposome-based intracellular delivery (Damayanti, Parker, & Irudayaraj, 2013; Kurzawa, Pellerano, & Morris, 2010; Shao et al., 2018).

Genetically encodable fluorescent protein-based biosensors are powerful molecular tools enabling the visualization of kinase activities in living cells with high spatial and temporal resolution (Bolbat & Schultz, 2017; Greenwald, Mehta, & Zhang, 2018; Maryu et al., 2018; Mehta & Zhang, 2021; Regot, Hughey, Bajar, Carrasco, & Covert, 2014; Zhou, Mehta, & Zhang, 2020). These biosensors can be transiently or stably expressed, and are thus highly suitable for quantitative imaging in living cells. For example, Kinase Translocation Reporters (KTR) involve a phosphorylation-dependent nucleocytoplasmic shuttling event, and the relative ratio of cytoplasmic versus nuclear fluorescence of the KTR is used as a proxy for cellular kinase activity (Kudo et al., 2018; Regot et al., 2014). As single-fluorophore sensors, KTRs are well suited for multiplex imaging, whereas FRET-based reporters require two fluorescent proteins with specific spectral properties, which narrows the options for multiplexing. The fluorescence readout of KTRs, however, is directly linked to their cytoplasmic or nuclear localization, thus restricting the spatial resolution of these

reporters and making them unsuitable for the applications described in this protocol. In contrast, the fluorescent readout from FRET-based reporters is independent of their localization, and FRET-based sensors can thus be targeted to various subcellular locations, such as the plasma membrane and the lysosome, providing detailed spatial information. For specifically measuring Akt activity, several genetically encodable biosensors have been developed, which serve as surrogate substrates of Akt and convert Akt-specific phosphorylation into a measurable fluorescent readout, such as redistribution of fluorescence from the nucleus to the cytosol (Gross & Rotwein, 2015, 2016; Maryu, Matsuda, & Aoki, 2016), or changes in FRET (Gao & Zhang, 2008; Kunkel, Ni, Tsien, Zhang, & Newton, 2005; Sasaki, Sato, & Umezawa, 2003; Zhou et al., 2015).

The herein provided protocols describe the use of a genetically encodable FRET-based biosensor, AktAR2 (Gao & Zhang, 2008, 2009; Zhou et al., 2015), which can be targeted to different subcellular localizations to assess location-specific Akt activity in living cells, a characteristic that is essential for Akt to control specific cellular functions. For example, using plasma membrane-targeted AktAR and an engineered voltage-controlled PTEN (phosphatase and tensin homologue), Mavrantoni et al detected in real time the rapid inhibition of Akt following activation of PTEN, a lipid phosphatase that depletes 3-phosphoinositides (3-PIs) (Mavrantoni et al., 2015). In addition, the use of targeted AktAR revealed that Akt activation, which depends on accumulation of 3-PIs, is faster and stronger within lipid rafts compared with nonraft regions of the plasma membrane (Gao & Zhang, 2008). Mislocalization of PTEN away from its primary nonraft distribution an into raft regions, either by genetic targeting or ceramide-induced recruitment, abolished Akt activity and inhibited proper functioning of the PI3K/Akt pathway (Gao et al., 2011). Furthermore, an allosteric lipid switch model for cellular Akt activation has been proposed, which suggested that phosphorylated, active Akt is restricted to 3-PI-containing membranes, and association with 3-PI prevents the dephosphorylation and deactivation of Akt (Ebner, Lucic, Leonard, & Yudushkin, 2017; Yudushkin, 2020). Using subcellularly targeted AktARs, we detected Akt activity at various membrane compartments (Chen et al., 2021; Gao & Zhang, 2008; Zhou, Zhong et al., 2020). In particular, 3-PIs, which predominantly accumulate at the plasma membrane, unexpectedly accumulate at the lysosomal membrane in response to growth factor stimulation, specifically promoting lysosomal Akt/mTOR signaling (Chen et al., 2021). However, robust Akt activity is also detected in the cytosol and in the nucleus (Chen et al., 2021; Zhou, Zhong et al., 2020), in addition to the plasma membrane and endomembrane surfaces. Whether there are alternative mechanisms for cellular Akt activation (Kunstle et al., 2002; Pekarsky et al., 2000) remains an important and active area of investigation. For example, phosphorylation of Ser477/Thr479 at the C-terminal tail of Akt by Cdk2/cyclinA2 (Liu et al., 2014) is suggested to interact with the PH domain to relieve autoinhibition (Chu et al., 2018). It has also been suggested that T-cell leukemia 1 (Tcl1) interacts with the pleckstrin homology (PH) domain of Akt, and this interaction leads to the enhancement of the Akt kinase activity (Kunstle et al., 2002; Laine, Kunstle, Obata, Sha, & Noguchi, 2000; Pekarsky et al., 2000), as well as the nuclear translocation of Akt (Pekarsky et al., 2001). We expect that AktARs will be useful molecular tools, in combination with biochemical or genetic perturbation, to test these different models.

AktARs can also be used to measure basal Akt kinase activity in cancer cells with PI3K, PTEN, or Akt mutations, by treating cells with Akt-specific inhibitors and quantifying the resulting decrease in the response of AktARs, an approach that has been used to probe the basal activities of other kinases, including protein kinase A (Depry, Allen, & Zhang, 2011), protein kinase C (Baffi, Van, Zhao, Mills, & Newton, 2019; Callender et al., 2018; Gallegos, Kunkel, & Newton, 2006), and mTORC1 (Zhou, Zhong et al., 2020). As an example, to assess the activity of Akt1 mutants in living cells, Balasuriya et al treated cells coexpressing Akt reporter (BKAR) and different Akt1 mutants with Akt inhibitor GDC-0068 following Akt activation, and they identified that T308D is not a constitutively active Akt1 mutant (Balasuriya et al., 2018).

We also provide a guide for controlling Akt activity at specific locations using Akt-STOPS. In contrast to pharmacological inhibition of Akt activity using small molecule drugs, Akt-STOPS can be subcellularly targeted to suppress Akt activity in a location-specific manner. Basic Protocol 1 provides steps for selective inhibition of plasma membrane and nuclear Akt activity using PM-Akt-STOPS and Akt-STOPS-NLS, respectively, with real-time tracking of local Akt activity simultaneously achieved using subcellularly targeted AktAR2, thus allowing the probing of compartment-specific Akt regulation and function (Zhou, Zhong et al., 2020). As an example, expressing nuclear Akt-STOPS in the nucleus significantly inhibits nuclear mTORC1 activity induced by growth factor and suppresses mTORC1-mediated pol III-dependent transcription, suggesting that the nuclear pool of Akt activity is critical for regulating nuclear mTORC1 activity and function (Zhou, Zhong et al., 2020). Furthermore, using CID-controlled Akt-STOPS, as in Basic Protocol 2, it is also possible to acutely inhibit Akt at the plasma membrane by rapidly recruiting Akt-STOPS to the site by rapamycin or rapalogs (which have high affinity and permeability) on a timescale of seconds to minutes (Fig. 3), compared to chronic inhibition by Akt-STOPS, which happens on a time scale of hours (Basic Protocol 1). The CID system opens up a new opportunity to capture dynamic signaling events following immediate suppression of highly localized Akt activity. For example, this system can be used to manipulate the dynamics of signaling events downstream of plasma membrane Akt, and this information can be combined with computational modeling to provide a quantitative understanding of signaling networks, such as cancer cell migration and invasion involving plasma membrane Akt activity.

CRITICAL PARAMETERS

Starvation of cells for imaging—The purpose of serum starvation is to reduce the basal phosphorylation of the reporter prior to stimulating Akt activity. Since overnight serum starvation lowers Akt activity (Franke et al., 1995), NIH3T3 cells expressing AktAR2 are typically imaged for PDGF-induced response following 21–24 hr of incubation in serum-free medium. Serum starvation may also be carried out in media containing a low serum concentration, typically 0.1–0.5%, and the time frame for serum starvation can vary widely among different cell types, sometimes as short as 30 min (Pirkmajer & Chibalin, 2011; Tan, You, Wu, Altomare, & Testa, 2010). Parameters for serum starvation should be optimized to reduce basal Akt activity in the cells to be studied.

Selecting suitable cells—Selecting suitable cells is important for successful imaging experiments. Generally, the criteria for selecting suitable cells include cell health, clear expression of Akt activity reporter and Akt-STOPS, and expected cellular distribution of the fluorescent signal. First, selecting healthy cells ensures that the results will be reproducible. Cells that are unhealthy will likely respond poorly and may detach from the dish during imaging; therefore, cell morphology should be inspected to confirm the health of the cells to be imaged. For example, healthy NIH3T3 cells should appear fibroblast-like and have elongated shapes, rather than being balled-up or rounded. Healthy Cos7 cells should appear flat and spread out. Second, select cells with intermediate-to-high fluorescence intensities. Too-high intensities due to overly high expression of the kinase reporter could raise the possibility of perturbation of endogenous signaling pathways and potential phototoxicity, whereas too-low intensities may lead to reduced signal-to-noise ratios, making it difficult to detect changes in FRET. Suitable cells with intermediate-to-high fluorescence intensities may exhibit 2%–13% of the dynamic range of the camera, depending on exposure times for the channel, ND filter(s) used, and camera setting. For example, for a camera sensor to respond with its maximum value of 60,000, select cells with intensity in the rough range of 1000 – 8000. Proper cellular distribution of fluorescence should also be examined. Diffusive AktAR2 and Akt-STOPS should exhibit uniform fluorescence throughout the cell, whereas the fluorescence of subcellularly targeted AktAR2 and Akt-STOPS should be limited only to the region of localization (Fig. 3A). Co-staining with a localization marker, such as Hoechst with AktAR2-NLS or Akt-STOPS-NLS, can be used to verify that correct targeting has been achieved.

Control experiments—It is important that control experiments be performed to validate that the responses of AktAR2 and inhibition by Akt-STOPS are specific for Akt. Specificity of AktAR2, including the untargeted and subcellularly targeted probes, can be examined by pretreating cells with Akt inhibitors, such as GDC-0068 or the allosteric inhibitor MK-2206, before stimulating the cells. These treatments should block the FRET response. Addition of the inhibitors following stimulation should lead to a reversal of the AktAR2 response. However, the reversal of the response may not be as robust as the blockade of response by pretreatment, depending on the cellular or subcellular phosphatase activities. Another negative control experiment is to use a reporter variant containing a T-to-A mutation (AktAR2-TA), wherein the phosphorylation site of the substrate peptide is mutated to a non-phosphorylatable alanine residue. This should also abrogate the reporter response. To examine the specificity of Akt-STOPS, negative control experiments include imaging AktAR2 in cells expressing mCherry alone or an mCherry-tagged scrambled peptide (Zhou, Zhong et al., 2020). In addition, biochemical characterization using *in vitro* kinase assays can be performed (Zhou, Zhong et al., 2020). Examining the effects of Akt-STOPS expression on the cellular activity of other kinases via live-cell imaging or immunoblotting can serve as control experiments as well (Zhou, Zhong et al., 2020).

TROUBLESHOOTING

Table 1 describes some potential areas where problems may arise during AktAR2 and Akt-STOPS experiments, along with possible causes and strategies for overcoming or avoiding these problems.

UNDERSTANDING RESULTS

For AktAR2 imaging, treatment with PDGF should produce an increase in the intensity of the FRET channel, along with a decrease in CFP channel intensity and, thus, an increase in the yellow-to-cyan emission ratio, if Akt activity is properly induced. Subsequent addition of Akt inhibitors GDC-0068 or MK-2206 should reverse the response (see Critical Parameters). Once Akt activity is detected at a defined location, Akt-STOPS can then be targeted to the same location. The local Akt activity can be measured concomitantly by AktAR2 to examine whether it is efficiently perturbed by Akt-STOPS. As a control, AktAR2 targeted to locations other than where Akt activity is being perturbed can be imaged to examine specificity.

We recommend at least two technical replicates per experiment, and independently repeating experiments across at least three different cell preparations per condition on different days. To generate the average response curves (Fig. 3B and 3D), pool the time course emission ratios (R/R_0) together, calculate the average emission ratio and standard error of the mean at each time point, and plot the data. Biosensor responses are calculated as the maximum ratio changes ($\Delta R/R_0$) after stimulation, and they are presented as percentage (%) (see step 13 in **Basic Protocol 1**). We have summarized our results of the PDGF-induced responses of AktAR2 targeted to the plasma membrane, cytosol, and nucleus in the absence and presence of expression of PM-Akt-STOPS (Fig. 3C) or Akt-STOPS-NLS (Fig. 3E) in serum-starved NIH3T3 cells. Next, pairwise comparisons, for example, comparing the AktAR2 responses to PDGF stimulation with or without Akt-STOPS expression, should be performed, using two-sided Student's t-test, or Welch's unequal variance t-test when sample sizes and variance are unequal between groups. Comparisons among three or more groups, for example, comparing AktAR2 responses among cells co-expressing mCherry, scrambled peptide, or Akt-STOPS, should be performed using ordinary one-way ANOVA followed by an appropriate multiple comparisons test. These tests should be applied to data that follows a Gaussian distribution. Otherwise, the corresponding non-parametric test (e.g., Mann-Whitney U-test or Kruskal-Wallis test) should be applied. As shown in Fig. 3C, Akt-STOPS-NLS shows efficient and selective inhibition of nuclear Akt activity, with little effects on cytosol or plasma membrane Akt activity. PM-Akt-STOPS shows efficient but less location-selective suppression of plasma membrane Akt activity (Fig. 3E), suggesting that nuclear Akt activity may have some dependence on plasma membrane Akt activity, possibly due to signal propagation from the plasma membrane to various intracellular compartments.

For CID-controlled Akt-STOPS, accumulation of red fluorescence at the cell periphery upon addition of rapamycin or rapalog should be observed within a few minutes, indicating successful induction of FKBP-Akt-STOPS translocation to the plasma membrane (Fig. 4C, upper panel; Movie 2). Accordingly, the response from PM-AktAR2 should decrease following addition of a dimerizer, as recruitment of FKBP-Akt-STOPS efficiently inhibits the plasma membrane activity of Akt (Fig. 4C, lower panel). The decrease in PM-AktAR2 response depends on both the dephosphorylation of the reporter by cellular phosphatases and inhibition by Akt-STOPS translocation, and we recommend imaging for about 20 min following addition of dimerizer to monitor the full reversal. Furthermore, since FKBP-Akt-STOPS initially localizes to the cytosol, it is expected that expression of FKBP-Akt-STOPS

may slightly change the slope of the PDGF-induced PM-AktAR2 response (Fig. 4C, lower panel), compared to the response of PM-AktAR2 expressed alone (Fig. 3B, blue curve). This is due to the close proximity of the cytosolic compartment to the plasma membrane and, therefore, potential interference with the accumulation of Akt activity at the plasma membrane by cytosolic FKBP-Akt-STOPS.

The CID system used in this study consists of $FKBP^{WT}$-Akt-STOPS and PM-FRB^{T2098L}. It has been shown that pretreatment with rapamycin (100 nM for 40 min) before PDGF stimulation in NIH3T3 cells had no discernable effect on the phosphorylation of Akt and ERK (Rahman & Haugh, 2017). Given that the same concentration was used in CID experiments and incubation was about 20 min, suppression of Akt activity following addition of rapamycin should be solely due to relocation of $FKBP^{WT}$-Akt-STOPS. If there is any concern, rapalog AP21967 should be used, which does not interfere with the endogenous FRB domain of mTOR (Bayle et al., 2006). We showed that AP21967 also rapidly induces the translocation of $FKBP^{WT}$-Akt-STOPS with comparable efficiency relative to rapamycin (Zhou et al., 2020).

Once the desired suppression of local Akt activity using Akt-STOPS is achieved, it is possible to investigate downstream signaling pathways that are dependent on the localized Akt activity to gain a deeper understanding of the specificity and coordination of the signaling network. This can be accomplished using the powerful and versatile toolkit of genetically encoded fluorescent reporters that have been developed to monitor various molecular and cellular processes, including dynamic changes in enzyme activity, protein-protein interactions, and intracellular levels of second messengers and metabolites (Greenwald et al., 2018; Mehta & Zhang, 2021). As an example, visualizing nuclear mTORC1 activity induced by growth factor using the nuclear-targeted FRET-based mTORC1 activity reporter (TORCAR) (Zhou et al., 2015) in the absence and presence of nuclear Akt-STOPS expression revealed that nuclear Akt activity is required for nuclear mTORC1 activity (Zhou, Zhong et al., 2020). In addition, CID-controlled Akt-STOPS, which showed rapid inhibition of Akt in a location-specific manner, is a robust tool and is expected to allow dissecting signaling networks or reconstitute complex signaling patterns in the future.

TIME CONSIDERATIONS

The time frames involved in the different sections of the protocols described in this article are stated within each protocol.

Supplementary Material

Refer to Web version on PubMed Central for supplementary material.

ACKNOWLEDGEMENTS:

This work was supported by NIH grants, R35 CA197622 and R01 DE030497 (J.Z.).

DATA AVAILABILITY STATEMENT:

The data that support this protocol are available from the corresponding author upon reasonable request.

LITERATURE CITED:

Baffi TR, Van AN, Zhao W, Mills GB, & Newton AC (2019). Protein Kinase C Quality Control by Phosphatase PHLPP1 Unveils Loss-of-Function Mechanism in Cancer. Mol Cell, 74(2), 378–392 e375. [PubMed: 30904392]

Balasuriya N, Kunkel MT, Liu X, Biggar KK, Li SS, Newton AC (2018). Genetic code expansion and live cell imaging reveal that Thr-308 phosphorylation is irreplaceable and sufficient for Akt1 activity. J Biol Chem, 293(27), 10744–10756. [PubMed: 29773654]

Bayle JH, Grimley JS, Stankunas K, Gestwicki JE, Wandless TJ, & Crabtree GR (2006). Rapamycin analogs with differential binding specificity permit orthogonal control of protein activity. Chem Biol, 13(1), 99–107. [PubMed: 16426976]

Bolbat A, & Schultz C (2017). Recent developments of genetically encoded optical sensors for cell biology. Biol Cell, 109(1), 1–23. [PubMed: 27628952]

Callender JA, Yang Y, Lorden G, Stephenson NL, Jones AC, Brognard J (2018). Protein kinase Calpha gain-of-function variant in Alzheimer's disease displays enhanced catalysis by a mechanism that evades down-regulation. Proc Natl Acad Sci U S A, 115(24), E5497–E5505. [PubMed: 29844158]

Chan TO, Rittenhouse SE, & Tsichlis PN (1999). AKT/PKB and other D3 phosphoinositide-regulated kinases: kinase activation by phosphoinositide-dependent phosphorylation. Annu Rev Biochem, 68, 965–1014. [PubMed: 10872470]

Chen M, Sun T, Zhong Y, Zhou X, & Zhang J (2021). A Highly Sensitive Fluorescent Akt Biosensor Reveals Lysosome-Selective Regulation of Lipid Second Messengers and Kinase Activity. ACS Cent Sci, 7(12), 2009–2020. [PubMed: 34963894]

Christopher JA, Geladaki A, Dawson CS, Vennard OL, & Lilley KS (2022). Subcellular Transcriptomics and Proteomics: A Comparative Methods Review. Mol Cell Proteomics, 21(2), 100186. [PubMed: 34922010]

Chu N, Salguero AL, Liu AZ, Chen Z, Dempsey DR, Ficarro SB (2018). Akt Kinase Activation Mechanisms Revealed Using Protein Semisynthesis. Cell, 174(4), 897–907 e814. [PubMed: 30078705]

Coutinho-Budd JC, Snider SB, Fitzpatrick BJ, Rittiner JE, & Zylka MJ (2013). Biological constraints limit the use of rapamycin-inducible FKBP12-Inp54p for depleting PIP2 in dorsal root ganglia neurons. J Negat Results Biomed, 12, 13. [PubMed: 24010830]

Damayanti NP, Parker LL, & Irudayaraj JM (2013). Fluorescence lifetime imaging of biosensor peptide phosphorylation in single live cells. Angew Chem Int Ed Engl, 52(14), 3931–3934. [PubMed: 23450802]

Depry C, Allen MD, & Zhang J (2011). Visualization of PKA activity in plasma membrane microdomains. Mol Biosyst, 7(1), 52–58. [PubMed: 20838685]

Dudak FC, Kilic N, Demir K, Yasar F, & Boyaci IH (2011). Enhancing the affinity of SEB-binding peptides by repeating their sequence. Biopolymers, 98(2), 145–154. [PubMed: 22733526]

Ebner M, Lucic I, Leonard TA, & Yudushkin I (2017). PI(3,4,5)P3 Engagement Restricts Akt Activity to Cellular Membranes. Mol Cell, 65(3), 416–431 e416. [PubMed: 28157504]

Franke TF, Kaplan DR, Cantley LC, & Toker A (1997). Direct regulation of the Akt proto-oncogene product by phosphatidylinositol-3,4-bisphosphate. Science, 275(5300), 665–668. [PubMed: 9005852]

Franke TF, Yang SI, Chan TO, Datta K, Kazlauskas A, Morrison DK (1995). The protein kinase encoded by the Akt proto-oncogene is a target of the PDGF-activated phosphatidylinositol 3-kinase. Cell, 81(5), 727–736. [PubMed: 7774014]

Gallegos LL, Kunkel MT, & Newton AC (2006). Targeting protein kinase C activity reporter to discrete intracellular regions reveals spatiotemporal differences in agonist-dependent signaling. J Biol Chem, 281(41), 30947–30956. [PubMed: 16901905]

Gao X, Lowry PR, Zhou X, Depry C, Wei Z, Wong GW (2011). PI3K/Akt signaling requires spatial compartmentalization in plasma membrane microdomains. Proc Natl Acad Sci U S A, 108(35), 14509–14514. [PubMed: 21873248]

Gao X, & Zhang J (2008). Spatiotemporal analysis of differential Akt regulation in plasma membrane microdomains. Mol Biol Cell, 19(10), 4366–4373. [PubMed: 18701703]

Gao X, & Zhang J (2009). Akt signaling dynamics in plasma membrane microdomains visualized by FRET-based reporters. Commun Integr Biol, 2(1), 32–34. [PubMed: 19704863]

Greenwald EC, Mehta S, & Zhang J (2018). Genetically Encoded Fluorescent Biosensors Illuminate the Spatiotemporal Regulation of Signaling Networks. Chem Rev, 118(24), 11707–11794. [PubMed: 30550275]

Gross SM, & Rotwein P (2015). Akt signaling dynamics in individual cells. J Cell Sci, 128(14), 2509–2519. [PubMed: 26040286]

Gross SM, & Rotwein P (2016). Mapping growth-factor-modulated Akt signaling dynamics. J Cell Sci, 129(10), 2052–2063. [PubMed: 27044757]

Inoue T, Heo WD, Grimley JS, Wandless TJ, & Meyer T (2005). An inducible translocation strategy to rapidly activate and inhibit small GTPase signaling pathways. Nat Methods, 2(6), 415–418. [PubMed: 15908919]

Kovarova M, Tolar P, Arudchandran R, Draberova L, Rivera J, & Draber P (2001). Structure-function analysis of Lyn kinase association with lipid rafts and initiation of early signaling events after Fcepsilon receptor I aggregation. Mol Cell Biol, 21(24), 8318–8328. [PubMed: 11713268]

Kudo T, Jeknic S, Macklin DN, Akhter S, Hughey JJ, Regot S (2018). Live-cell measurements of kinase activity in single cells using translocation reporters. Nat Protoc, 13(1), 155–169. [PubMed: 29266096]

Kulkarni GV, & McCulloch CA (1994). Serum deprivation induces apoptotic cell death in a subset of Balb/c 3T3 fibroblasts. J Cell Sci, 107 (Pt 5), 1169–1179. [PubMed: 7929626]

Kunkel MT, Ni Q, Tsien RY, Zhang J, & Newton AC (2005). Spatio-temporal dynamics of protein kinase B/Akt signaling revealed by a genetically encoded fluorescent reporter. J Biol Chem, 280(7), 5581–5587. [PubMed: 15583002]

Kunstle G, Laine J, Pierron G, Kagami Si S, Nakajima H, Hoh F (2002). Identification of Akt association and oligomerization domains of the Akt kinase coactivator TCL1. Mol Cell Biol, 22(5), 1513–1525. [PubMed: 11839817]

Kurzawa L, Pellerano M, & Morris MC (2010). PEP and CADY-mediated delivery of fluorescent peptides and proteins into living cells. Biochim Biophys Acta, 1798(12), 2274–2285. [PubMed: 20188697]

Laine J, Kunstle G, Obata T, Sha M, & Noguchi M (2000). The protooncogene TCL1 is an Akt kinase coactivator. Mol Cell, 6(2), 395–407. [PubMed: 10983986]

Lambert TJ (2019). FPbase: a community-editable fluorescent protein database. Nat Methods, 16(4), 277–278. [PubMed: 30886412]

Liu P, Begley M, Michowski W, Inuzuka H, Ginzberg M, Gao D (2014). Cell-cycle-regulated activation of Akt kinase by phosphorylation at its carboxyl terminus. Nature, 508(7497), 541–545. [PubMed: 24670654]

Lukovic E, Gonzalez-Vera JA, & Imperiali B (2008). Recognition-domain focused chemosensors: versatile and efficient reporters of protein kinase activity. J Am Chem Soc, 130(38), 12821–12827. [PubMed: 18759402]

Mabe S, Nagamune T, & Kawahara M (2014). Detecting protein-protein interactions based on kinase-mediated growth induction of mammalian cells. Sci Rep, 4, 6127. [PubMed: 25135216]

Maiuri T, Ho J, & Stambolic V (2010). Regulation of adipocyte differentiation by distinct subcellular pools of protein kinase B (PKB/Akt). J Biol Chem, 285(20), 15038–15047. [PubMed: 20223817]

Manning BD, & Toker A (2017). AKT/PKB Signaling: Navigating the Network. Cell, 169(3), 381–405. [PubMed: 28431241]

Maryu G, Matsuda M, & Aoki K (2016). Multiplexed Fluorescence Imaging of ERK and Akt Activities and Cell-cycle Progression. Cell Struct Funct, 41(2), 81–92. [PubMed: 27247077]

Maryu G, Miura H, Uda Y, Komatsubara AT, Matsuda M, & Aoki K (2018). Live-cell Imaging with Genetically Encoded Protein Kinase Activity Reporters. Cell Struct Funct, 43(1), 61–74. [PubMed: 29553079]

Mavrantoni A, Thallmair V, Leitner MG, Schreiber DN, Oliver D, & Halaszovich CR (2015). A method to control phosphoinositides and to analyze PTEN function in living cells using voltage sensitive phosphatases. Front Pharmacol, 6, 68. [PubMed: 25873899]

Mehta S, & Zhang J (2021). Biochemical Activity Architectures Visualized-Using Genetically Encoded Fluorescent Biosensors to Map the Spatial Boundaries of Signaling Compartments. Acc Chem Res, 54(10), 2409–2420. [PubMed: 33949851]

Miura H, Matsuda M, & Aoki K (2014). Development of a FRET biosensor with high specificity for Akt. Cell Struct Funct, 39(1), 9–20. [PubMed: 24212374]

Mori Y, Yoshida Y, Satoh A, & Moriya H (2020). Development of an experimental method of systematically estimating protein expression limits in HEK293 cells. Sci Rep, 10(1), 4798. [PubMed: 32179769]

Nhu Ngoc Van T, & Morris MC (2013). Fluorescent sensors of protein kinases: from basics to biomedical applications. Prog Mol Biol Transl Sci, 113, 217–274. [PubMed: 23244792]

Pekarsky Y, Hallas C, Palamarchuk A, Koval A, Bullrich F, Hirata Y (2001). Akt phosphorylates and regulates the orphan nuclear receptor Nur77. Proc Natl Acad Sci U S A, 98(7), 3690–3694. [PubMed: 11274386]

Pekarsky Y, Koval A, Hallas C, Bichi R, Tresini M, Malstrom S (2000). Tcl1 enhances Akt kinase activity and mediates its nuclear translocation. Proc Natl Acad Sci U S A, 97(7), 3028–3033. [PubMed: 10716693]

Pirkmajer S, & Chibalin AV (2011). Serum starvation: caveat emptor. Am J Physiol Cell Physiol, 301(2), C272–279. [PubMed: 21613612]

Regot S, Hughey JJ, Bajar BT, Carrasco S, & Covert MW (2014). High-sensitivity measurements of multiple kinase activities in live single cells. Cell, 157(7), 1724–1734. [PubMed: 24949979]

Ross B, Mehta S, & Zhang J (2017). Molecular tools for acute spatiotemporal manipulation of signal transduction. Curr Opin Chem Biol, 34, 135–142.

Sasaki K, Sato M, & Umezawa Y (2003). Fluorescent indicators for Akt/protein kinase B and dynamics of Akt activity visualized in living cells. J Biol Chem, 278(33), 30945–30951. [PubMed: 12773546]

Shao S, Li Z, Cheng H, Wang S, Perkins NG, Sarkar P (2018). A Chemical Approach for Profiling Intracellular AKT Signaling Dynamics from Single Cells. J Am Chem Soc, 140(42), 13586–13589. [PubMed: 30351133]

Shults MD, Carrico-Moniz D, & Imperiali B (2006). Optimal Sox-based fluorescent chemosensor design for serine/threonine protein kinases. Anal Biochem, 352(2), 198–207. [PubMed: 16600168]

Shults MD, Janes KA, Lauffenburger DA, & Imperiali B (2005). A multiplexed homogeneous fluorescence-based assay for protein kinase activity in cell lysates. Nat Methods, 2(4), 277–283. [PubMed: 15782220]

Sugiyama MG, Fairn GD, & Antonescu CN (2019). Akt-ing Up Just About Everywhere: Compartment-Specific Akt Activation and Function in Receptor Tyrosine Kinase Signaling. Frontiers in Cell and Developmental Biology, 7.

Tan Y, You H, Wu C, Altomare DA, & Testa JR (2010). Appl1 is dispensable for mouse development, and loss of Appl1 has growth factor-selective effects on Akt signaling in murine embryonic fibroblasts. J Biol Chem, 285(9), 6377–6389. [PubMed: 20040596]

Voss S, Klewer L, & Wu YW (2015). Chemically induced dimerization: reversible and spatiotemporal control of protein function in cells. Curr Opin Chem Biol, 28, 194–201. [PubMed: 26431673]

Waters JC (2009). Accuracy and precision in quantitative fluorescence microscopy. J Cell Biol, 185(7), 1135–1148. [PubMed: 19564400]

Yamaguchi H, Yoshida S, Muroi E, Yoshida N, Kawamura M, Kouchi Z (2011). Phosphoinositide 3-kinase signaling pathway mediated by p110alpha regulates invadopodia formation. J Cell Biol, 193(7), 1275–1288. [PubMed: 21708979]

Yudushkin I (2020). Control of Akt activity and substrate phosphorylation in cells. IUBMB Life, 72(6), 1115–1125. [PubMed: 32125765]

Zhou X, Clister TL, Lowry PR, Seldin MM, Wong GW, & Zhang J (2015). Dynamic Visualization of mTORC1 Activity in Living Cells. Cell Rep, 10(10), 1767–1777. [PubMed: 25772363]

Zhou X, Mehta S, & Zhang J (2020). Genetically Encodable Fluorescent and Bioluminescent Biosensors Light Up Signaling Networks. Trends Biochem Sci, 45(10), 889–905. [PubMed: 32660810]

Zhou X, Zhong Y, Molinar-Inglis O, Kunkel MT, Chen M, Sun T (2020). Location-specific inhibition of Akt reveals regulation of mTORC1 activity in the nucleus. Nat Commun, 11(1), 6088. [PubMed: 33257668]

KEY REFERENCES:

Zhou X, Zhong Y, Molinar-Inglis O, Kunkel MT, Chen M, Sun T (2020). Location-specific inhibition of Akt reveals regulation of mTORC1 activity in the nucleus. Nat Commun, 11(1), 6088. Describing the development and characterization of Akt-STOPS. [PubMed: 33257668]

Gao X, & Zhang J (2008). Spatiotemporal analysis of differential Akt regulation in plasma membrane microdomains. Mol Biol Cell, 19(10), 4366–4373. Describing the development and characterization of AktAR, from which AktAR2 was optimized. [PubMed: 18701703]

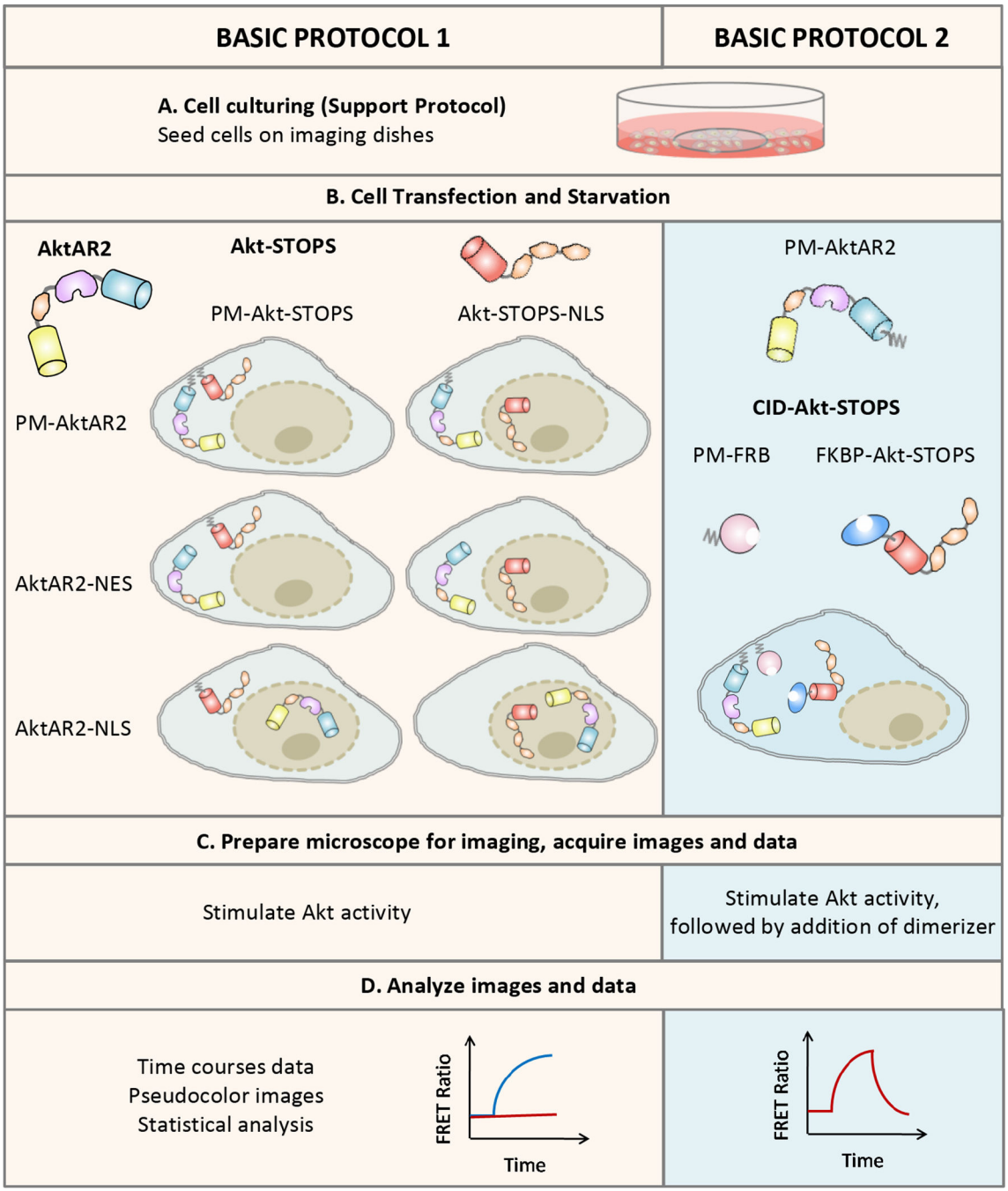

Figure 1.

Overview of the experimental workflow described in this article. (Left) Basic Protocol 1 describes the steps for visualizing and perturbing subcellular Akt kinase activity using AktAR2 and Akt-STOPS. (Right) Basic Protocol 2 describes the steps for using chemically inducible dimerization-controlled Akt-STOPS to exert temporal control over the location-specific inhibition of Akt signaling. See text for details.

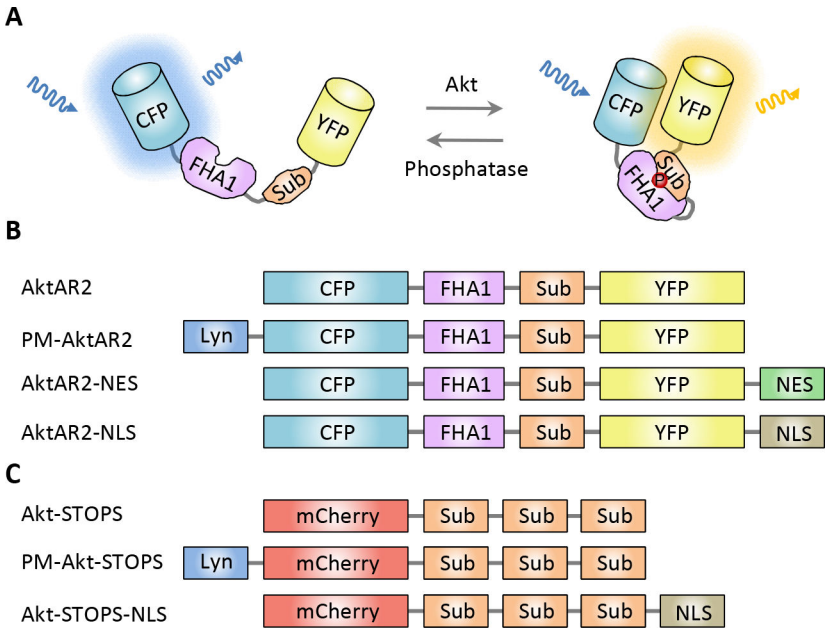

Figure 2.

Subcellularly targeted AktAR2 and Akt-STOPS. (**A**) Akt phosphorylates the substrate peptide (sub) derived from Forkhead Box O1 (FoxO1) in AktAR2, resulting in intramolecular binding by an FHA1 phosphoamino acid binding domain. The resulting conformational change leads to an increase in the proximity between cyan (CFP) and yellow fluorescent protein (YFP), which can be read out as a change in the yellow-to-cyan emission ratio. (**B**) Domain structures of AktAR2 constructs used in this study. From top to bottom, diffusive AktAR2, plasma membrane-targeted AktAR2 (PM-AktAR2), cytosolic AktAR2 (AktAR2-NES), and nuclear AktAR2 (AktAR2-NLS). AktAR2 is composed of CFP, the phosphoamino acid binding domain FHA1, an Akt substrate peptide, and YFP. PM-AktAR2 is generated by fusing a Lyn kinase targeting motif to the N-terminus of AktAR2. Attaching a nuclear localization signal (NLS) or a nuclear export signal (NES) to the C-terminus of AktAR2 generates the nuclear (AktAR2-NLS) and cytosolic AktAR2 (AktAR2-NES), respectively. (**C**) Domain structures of Akt-STOPS constructs used in this study. From top to bottom, diffusive Akt-STOPS, plasma membrane-targeted Akt-STOPS (PM-Akt-STOPS), and nuclear AktAR2 (Akt-STOPS-NLS). Akt-STOPS was generated by attaching three tandem repeats of an Akt substrate peptide to the C-terminus of a red fluorescent protein (mCherry). Three repeating sequences of the substrate peptide allows the peptide to adopt multiple conformations and increases the number of putative binding spots to facilitate binding to active Akt. PM-Akt-STOPS is generated by fusing a Lyn kinase targeting motif to the N-terminus. Attaching a nuclear localization signal (NLS) to the C-terminus of Akt-STOPS generates the nuclear Akt-STOPS (Akt-STOPS-NLS).

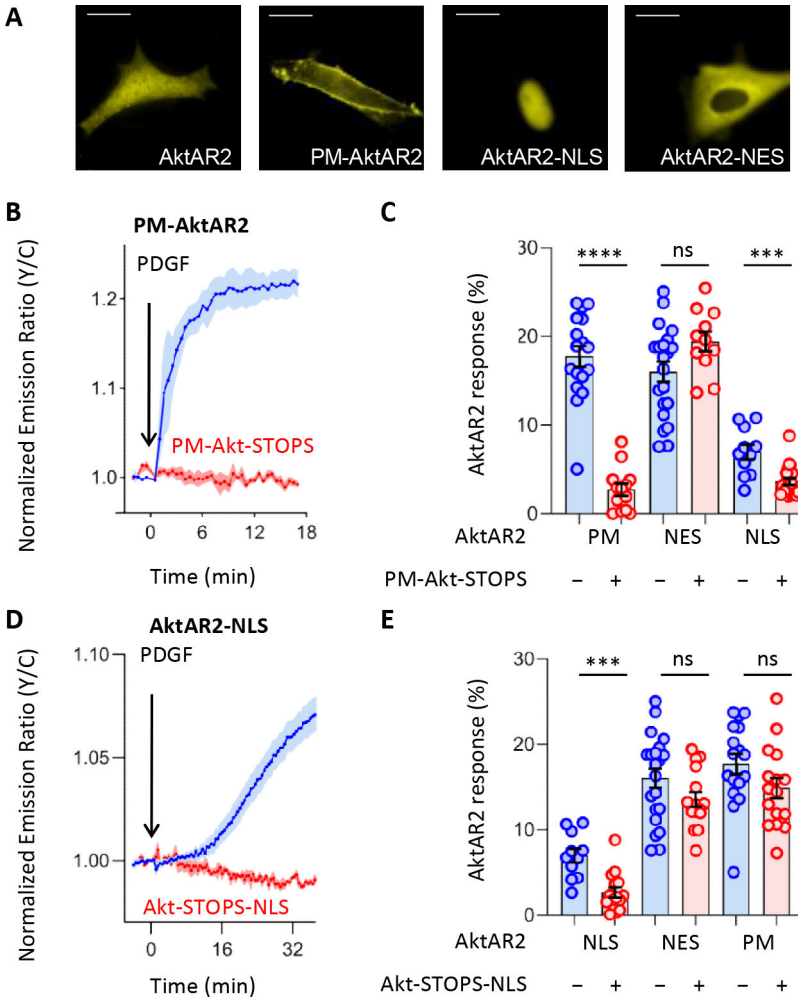

Figure 3.

Visualizing and perturbing subcellular Akt kinase activity using AktAR and Akt-STOPS. (**A**) Sample images showing serum-starved NIH3T3 cells expressing diffusive AktAR2, plasma membrane-targeted AktAR2 (PM-AktAR2), nuclear AktAR2 (AktAR2-NLS), and cytosolic AktAR2 (AktAR2-NES). Scale bar = 10 μm. (**B**) Average time courses of the normalized yellow-to-cyan (Y/C) emission ratio (R/R_0) in serum-starved NIH3T3 cells expressing PM-AktAR2 without (blue, n = 17) or with (red, n = 13) PM-Akt-STOPS expression. (**C**) Responses of PDGF-treated serum-starved NIH3T3 cells expressing subcellularly targeted AktAR2 with or without PM-Akt-STOPS expression. From left to right, responses of PM-AktAR2 without (n = 17) and with PM-Akt-STOPS expression (n = 13), unpaired two-tailed student's t-test with Welch's correction, ****, $p<0.0001$; responses of AktAR2-NES without (n = 21) and with PM-Akt-STOPS expression (n = 11), unpaired two-tailed student's t-test, ns, not significant, $p=0.1$; responses of AktAR2-NLS without (n = 11) and with PM-Akt-STOPS expression (n = 19), unpaired two-tailed student's t-test, ***, $p<0.001$. (**D**) Average time courses of the normalized Y/C emission ratio in serum-starved NIH3T3 cells expressing AktAR2-NLS without (blue, n = 11) or with (red, n = 15) PM-Akt-STOPS expression. (**E**) Responses of PDGF-treated serum-starved NIH3T3 cells expressing subcellularly targeted AktAR2 with or without Akt-STOPS-NLS expression. From left to

right, responses of AktAR2-NLS without (n = 11) and with Akt-STOPS-NLS expression (n = 15), unpaired two-tailed student's t-test, ***, $p<0.001$; responses of AktAR2-NES without (n = 21) and with Akt-STOPS-NLS expression (n = 16), unpaired two-tailed student's t-test, ns, not significant, $p=0.1$; responses of PM-AktAR2 without (n = 17) and with Akt-STOPS-NLS expression (n = 16), unpaired two-tailed student's t-test, ns, not significant, $p=0.1$. Solid lines in (B, D) indicate mean responses; shaded areas, SEM. Bars denote mean ± SEM (C, E). n numbers represent number of cells (Zhou, Zhong et al., 2020).

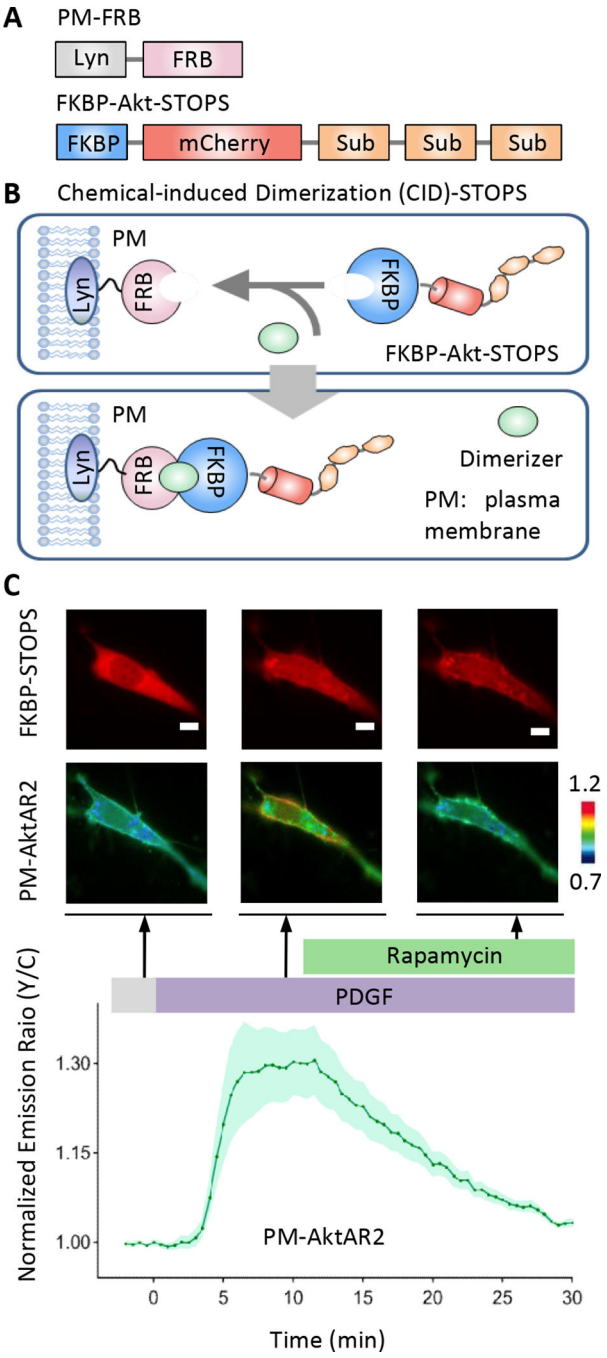

Figure 4.

Chemically Inducible Dimerization (CID)-controlled Akt-STOPS. (**A**) Domain structures of the two components of CID-Akt-STOPS based on dimerization between FK506 binding protein (FKBP) and FKBP12-rapamycin binding domain (FRB) that recruits Akt-STOPS to the plasma membrane. As a recruiter, FRB is targeted to the plasma membrane using a targeting motif derived from Lyn kinase (PM-FRB). Akt-STOPS is tagged with FKBP (FKBP-Akt-STOPS). (**B**) Cartoon depicting the dimerizer-induced translocation of Akt-STOPS to the plasma membrane. To inhibit plasma membrane Akt activity using CID, cells

expressing FKBP-Akt-STOPS and the plasma membrane recruiter PM-FRB are treated with the dimerizer. Addition of the dimerizer, either rapamycin or rapalog, induces formation of the FKBP-FRB heterodimer, which rapidly recruits Akt-STOPS and inhibits Akt activity at the plasma membrane. (**C**) Upper panel, representative images of serum-starved NIH3T3 cells expressing CID-Akt-STOPS, (PM-FRB and FKBP-Akt-STOPS). Scale bar = 10 μm. Lower panel, average time course of the normalized Y/C emission ratio (R/R_0) in serum-starved NIH3T3 expressing PM-AktAR2 and CID-Akt-STOPS (n = 7). Solid line in lower panel indicates the mean response; shaded area, SEM. n number represents number of cells (Zhou, Zhong et al., 2020).

Table 1

Troubleshooting.

Problem	Possible causes	Possible solutions
Dim cells	Poor transfection	Optimize transfection methods for the chosen cells, for example, increase the amount of plasmid DNA and the transfection reagents, improve the expression by incubating the cells for longer time after transfection, use different transfection reagents, or generate viral vectors for viral transduction (see also Strategic Planning).
	Incorrect filter set	Verify microscope filters
Unstable baseline	Changes in cell morphology	Optimize imaging conditions (e.g. image cells at 37°C, or change to FluoroBrite DMEM-based imaging buffer)
	Photobleaching	Reduce exposure time or decrease the illumination using neutral density filters
Smaller[a]**/slower**[b] **responses than expected**	Incorrect drug addition	Mix well or use a perfusion system
	Drug concentration too low	Use higher dose of drug, verify amount of drug needed to fully activate kinase in the chosen cells by immunoblotting, check the expression level of growth factor receptor if using growth factor as stimulation.
	Low expression of reporter	Optimize transfection methods for the chosen cells. See above
	High basal activity	Optimize starvation conditions, for example, check the phosphorylation of Akt substrates under different starvation conditions (serum concentrations and duration) by immunoblotting as an indication of basal activity
Little inhibition of AktAR2 response by Akt-STOPS	Low expression of Akt-STOPS	Increase the amount of plasmid DNA for Akt-STOPS for transfection, or select cells that express high levels of Akt-STOPS by setting a threshold for red fluorescence intensity.
No recruitment of FKBP-Akt-STOPS to the plasma membrane	Drug concentration too low	Use a higher dose of the drug to induce the dimerization and examine whether it efficiently induces an increase of red fluorescence at the plasma membrane.
	Low expression of PM-FRB	Optimize transfection by changing the amount of DNA and increasing the ratio of PM-FRB/FKBP-Akt-STOPS for transfection
	High expression of endogenous FKBP in the chosen cell line	Some cell types expressing large amounts of FKBP or FRB may limit the use of the rapamycin-induced dimerization system, for example, dorsal root ganglia neurons (Coutinho-Budd, Snider, Fitzpatrick, Rittiner, & Zylka, 2013). If that's the case, change to cell lines that have low endogenous FKBP12 or FRB, or use another CID system (Voss et al., 2015).

[a] No discernable response or less than 5% response for diffusive AktAR2, for example, or longer than 15 min for the onset of response.

[b] Subcellularly targeted AktAR2 may have varied dynamic range and kinetics.